Contribution from the Department of Chemistry,
Northeastern University, Boston, Massachusetts 02115,
Francis Bitter National Magnet Laboratory, Massachusetts
Institute of Technology, Cambridge, Massachusetts 02139,
and Department of Chemistry, University of North Carolina,
Chapel Hill, North Carolina 27514

Electronic Structure of Metal Cluster Compounds: A Magnetic Susceptibility and High-Field Mössbauer Spectroscopy Study of Cubane-Cluster Systems, $[(\eta^5\text{-}C_5H_5)FeS]_4{}^{n+}$ (n = 0, 1, 2)

Herbert Wong, Diana Sedney, William Michael Reiff,*
Richard B. Frankel, Thomas J. Meyer, and Dennis Salmon

Received July 8, 1977

X-ray determinations[1,2] of the structure of the nonheme, iron–sulfur proteins containing four iron atoms per molecule show that the iron sites have approximate tetrahedral symmetry with three sulfide and one cysteinyl sulfur ligand. The iron–sulfur tetrahedra are packed into a distorted cubic cluster with one sulfide bridging three iron atoms. This $[(\text{Cys–S})_4Fe_4S_4]$ cubane arrangement can exist in several oxidation states, with the electrons involved in the oxidation and reduction steps coming from and entering delocalized molecular orbitals that are centered on all four iron atoms and with all four iron atoms electronically equivalent in the oxidation state, corresponding to a reduced high-potential iron protein from *Chromatium*[3] and oxidized bacterial ferredoxin from *Peptococus Aerogenes*.[4,5]

Several complexes are known to have a cubane structure analogous to the active sites of the proteins.[6] These include $[(\eta^5\text{-}C_5H_5)FeS]_4{}^{n+}$ (n = 0, 1, 2),[7] hereafter designated I, II, and III respectively (Figure 1), which possesses the Fe_4S_4 "cubane core"; $[(\eta^5\text{-}C_5H_5)Fe(CO)]_4{}^{n+}$ (n = 0, 1),[8] also a tetrametal cluster but with CO groups replacing the bridging sulfides; and certain dithiolene complexes of the form $[(CF_3)_2C_2S_2FeS]_4{}^{n-}$ (n = 0, 1, 2),[9,10] which also contain an Fe_4S_4 core but with five sulfur atoms coordinated to each iron. Recently, complexes of the type $[(SR)FeS]_4{}^{2-}$, where SR is a simple alkyl or aryl mercaptide, have been shown[11-15] by a variety of physical and chemical techniques to be close structural and electronic analogues of the proteins.

A basic question for all the foregoing compounds is the influence of the ligands on the electronic and magnetic properties of the tetrametal core. Another important question is the nature of the molecular orbital involved in oxidation and reduction steps and its relation to the core. Experimentally, Mössbauer spectroscopy distinguishes different cases. In one case, the change in oxidation state is accompanied by significant changes in the isomer shift, quadrupole interaction, and magnetic hyperfine interaction at the iron sites. This is observed in the reduction of $[(SR)FeS]_4{}^{2-}$ to the trianion.[16] In another case, the change of oxidation state is accompanied by no or minimal changes in the Mössbauer parameters. This is observed in certain dithiolene tetrametal clusters.[10,17] In the former instance, the molecular orbital involved in the oxidation–reduction process can be described as tetrametal based, whereas in the second case it can be described as predominantly ligand based. An intermediate situation is observed in $[(\eta^5\text{-}C_5H_5)FeCO]_4$ where oxidation to the monocation results in a change in the quadrupole interaction and a small magnetic hyperfine interaction but no change in the isomer shift.[18,19]

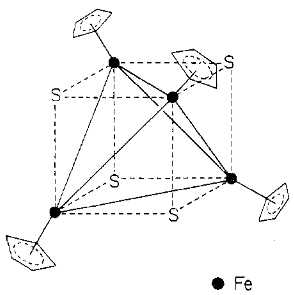

Figure 1. Schematic representation of the $[(\eta^5\text{-}C_5H_5)FeS]_4$ cluster.

In this paper, we extend the study of tetrametal cubane systems by variable-temperature susceptibility measurements and high-field Mössbauer spectroscopy to compounds I, II, and III. This allows a comparison of the effects of "innocent" terminal ligands, such as the mercaptides in $[FeS(SR)]_4{}^{n-}$, with "noninnocent" terminal ligands, such as cyclopentadienyl, on the electronic properties of the cubane Fe–S core. In the present series, I is a 20-core electron system from four formal iron(III) atoms, III is also an even-electron system with 18, while II contains 19-core electrons and must be paramagnetic. One of the aims of this study is to ascertain the nature of the molecular orbital occupied by the unpaired electron in II. The molecular structures of I, II, and III have recently been reported.[7,20,21]

Experimental Section

$[(\eta^5\text{-}C_5H_5)FeS]_4$ was prepared by the method of Wei et al.[7]

Preparation of $[(\eta^5\text{-}C_5H_5)FeS]_4PF_6$. A 500-mg amount of $[(\eta^5\text{-}C_5H_5)FeS]_4$ was suspended in 250 mL of 0.1 M ammonium hexafluorophosphate (AH) solution at 80 °C and oxidized at +0.45 V vs. SSCE at a platinum electrode until the current was 5% of its initial value (n = 0.74). The solution was filtered and evaporated, and the residue was washed with water to remove supporting electrolyte. The product was dissolved in a minimum amount of acetone, filtered, precipitated from solution by the addition of diethyl ether, and air-dried to yield 300 mg (49%) of $[(\eta^5\text{-}C_5H_5)FeS]_4PF_6$.

Anal. Calcd for $H_{20}C_{20}Fe_4S_4PF_6$: C, 31.90; H, 2.60. Found: C, 31.98; H, 2.70.

Preparation of $[(\eta^5\text{-}C_5H_5)FeS]_4(PF_6)_2$. A 150-mg amount of $[(\eta^5\text{-}C_5H_5)FeS]_4PF_6$ was dissolved in 250 mL of 0.1 M AH–acetonitrile solution and oxidized at +1.10 V vs. SSCE (n = 0.95). The solution was filtered and evaporated, and the residue was washed with water to remove AH. The product was washed several times with CH_2Cl_2 to remove any of the monocation $[(\eta^5\text{-}C_5H_5)FeS]_4PF_6$, then redissolved in CH_3CN, precipitated from solution by the addition of diethyl ether, and air-dried to yield 140 mg (78%) of $[(\eta^5\text{-}C_5H_5)FeS]_4(PF_6)_2$.

Anal. Calcd for $H_{20}C_{20}Fe_4S_4P_2F_{12}$: C, 26.60; H, 2.22. Found: C, 26.74; H, 2.13.

Mössbauer spectra were obtained using conventional constant acceleration spectrometers employing 100 mCi of ^{57}Co on rhodium as a source. Spectra in external fields were determined using a superconducting solenoid with longitudinal geometry. Both the source and absorber were at 4.2 K but with a fringing field at the source of less than 500 G. Fresh samples were used as absorbers and stored in liquid nitrogen between runs.

Variable-temperature **magnetic susceptibility** measurements were made at Northeastern University on a Faraday balance composed of a Cahn RG electrobalance, a Varian Model 4000 electromagnet with 4-in. constant-force pole caps, and a Janis Super Vari-Temp cryostat over the range 1.5 to 300 K for ten fields between 1.6 and 5 kG. Temperature measurement and control were typically of the order ±0.01 K or better and were achieved using a Leeds-Northrup K-5 potentiometer and a Lake Shore Cryotronics Model DT-500 C set point controller, respectively, in conjunction with a calibrated silicon temperature sensor diode, a 10-μA constant current source, and an uncalibrated gallium arsenide control diode. Final temperature equilibration and stability were continuously monitored on a Leeds-Northrup Speedomax-XL 600 mV recorder that was used to read the error signal of the calibrated silicon diode after cancellation by the K-5 potentiometer. Temperatures below 4.2 K were measured via the vapor pressure of helium using Wallace-Tiernan Models FA-160 and 61-050 absolute pressure gauges, while pumping was precisely controlled with an L. J. Engineering Model 329 vacuum

---

* To whom correspondence should be addressed at Northeastern University.

0020-1669/78/1317-0194$01.00/0

Table I. Mössbauer Data[a] (77 K) for Some Tetrametal Cluster Systems

Compd	δ, mm/s	ΔE, mm/s	Ref
$[(\eta^5\text{-}C_5H_5)FeS]_4$	0.30–0.35	0.95–1.15	This work
$[(\eta^5\text{-}C_5H_5)FeS]_4PF_6$	0.35	1.20	This work
$[(\eta^5\text{-}C_5H_5)FeS]_4(PF_6)_2$	0.35	1.20	This work
$[(\eta^5\text{-}C_5H_5)FeCO]_4$	0.40[b]	1.76	18
$[(\eta^5\text{-}C_5H_5)FeCO]_4Cl$	0.41[b]	1.40	18
$Fe_4S_4[S_2C_2(CF_3)_2]_4$	0.13	1.67	10
$Ph_4As\{Fe_4S_4[S_2C_2(CF_3)_2]_4\}$	0.17	1.62	10
$\{Ph_4As\}_2\{Fe_4S_4[S_2C_2(CF_3)_2]_4\}$	0.19	1.66	10
$[Et_4N]_2\{(PhCH_2S)FeS\}_4$	0.34	1.26	11
$\{(PhCH_2S)FeS\}_3{}^{3-}$ [c]	0.46	1.15	15, 16

[a] Relative to natural iron metal. [b] Obtained by subtracting 0.26 mm/s from δ relative to $Na_2Fe(CN)_5NO\cdot 2H_2O$. [c] Generated in solution.

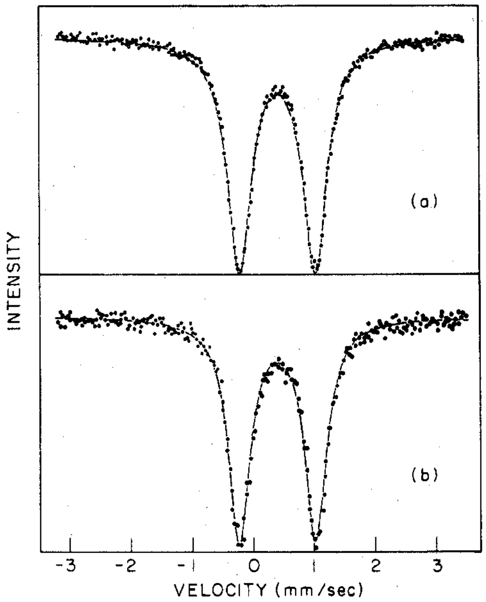

Figure 2. Zero-field Mössbauer spectra of $[(\eta^5\text{-}C_5H_5)FeS]_4PF_6$ (a) and $[(\eta^5\text{-}C_5H_5)FeS]_4(PF_6)_2$ (b) at 77 K. The curves are least-square fits assuming a single Lorentzian peak for each component of the quadrupole doublet.

regulator valve. Temperatures below 78 K and to as low as 50 K were also achieved using liquid nitrogen by pumping (Welch 1397) to well below the triple point on solid nitrogen. Both the vapor pressure of nitrogen and a calibrated silicon diode were used to monitor the temperature. An F. W. Bell Model 610 Gaussmeter with a transverse Hall probe was used for measurement of magnetic fields. The balance was calibrated with $HgCo(NCS)_4$. For measurements at $T < 50$ K, smaller sample weights were used. Measurements were made on several fresh samples of II and III with consistent results. Older samples of III, which had been stored at room temperature, were found to exhibit higher effective moments at 300 K, indicating various degrees of decomposition.

Results

Mössbauer Spectroscopy. Mössbauer spectra of compounds II and III consist of single, symmetric quadrupole doublets from 4.2 K to room temperature. The parameters are listed in Table I along with representative values for the other clusters listed in the introduction. Zero-field spectra of II and III at 78 K are given in Figure 2. As seen in Figure 3, the spectrum of I consists of superimposed quadrupole doublets, and there is no unambiguous way of assigning the spectral transitions to the neutral species and impurity. We thus report a range of possible isomer shift and quadrupole splittings in Table I for species I. We interpret the quadrupole doublet to be due to I, and the additional lines to impurities in the sample. Wei et al.[7] also noted difficulties in obtaining pure samples of I. Because of obvious impurity content, detailed magnetic field Mössbauer and susceptibility measurements were not made on I.

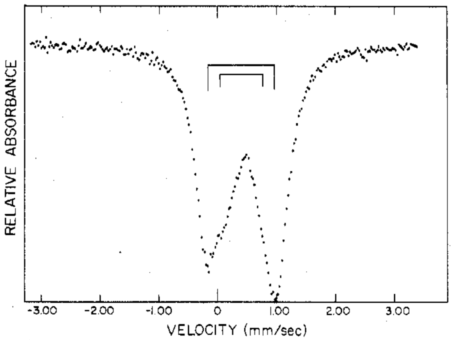

Figure 3. Zero-field Mössbauer spectrum of the neutral cluster $[(\eta^5\text{-}C_5H_5)FeS_4]$ at 77 K.

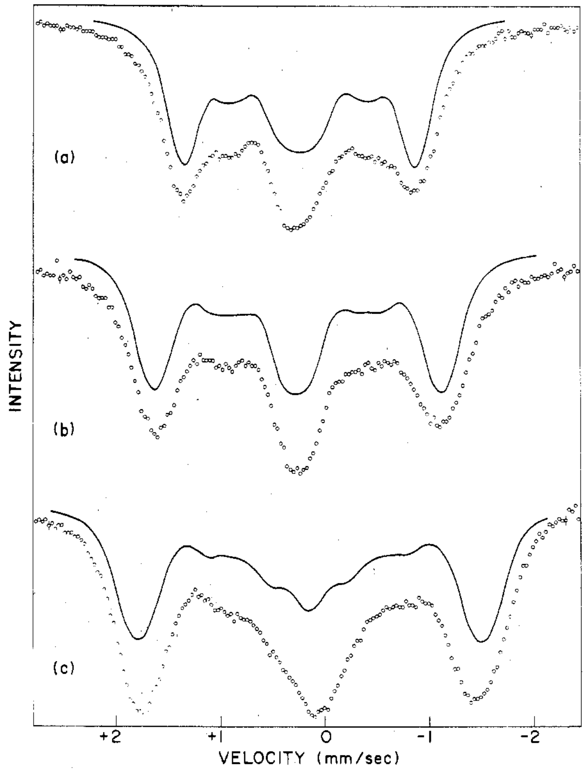

Figure 4. Mössbauer spectra of $[(\eta^5\text{-}C_5H_5)FeS]_4PF_6$ at 4.2 K in longitudinal magnetic fields of (a) 40 kG, (b) 60 kG, and (c) 80 kG. The solid lines are theoretical assuming $H_n = H_0$.

The field dependence of the spectrum of II up to 80 kG is shown in Figure 4. The spectrum of III is virtually identical. We have included computer-generated spectra (solid line) assuming a field at the nucleus $H_n = H_0$, a total quadrupole splitting of 1.20 mm/s (measured at $H = 0$, 4.2 K), and asymmetry parameter $\eta = 1.0$. Close inspection of the experimental data shows that the spectra are not quite sym-

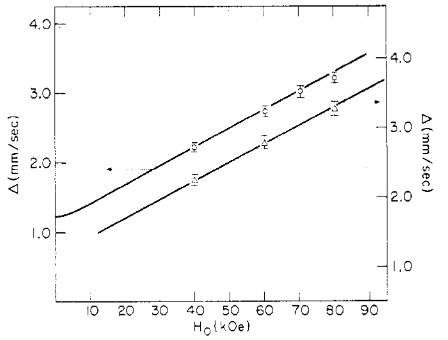

Figure 5. The outer line splitting plotted as a function of applied field: (O) $[(\eta^5\text{-}C_5H_5)FeS]_4PF_6$; (Δ) $[(\eta^5\text{-}C_5H_5)FeS]_4(PF_6)_2$. The scales have been separated for clarity. The solid lines correspond to the splittings obtained in computer simulations assuming $H_n = H_0$.

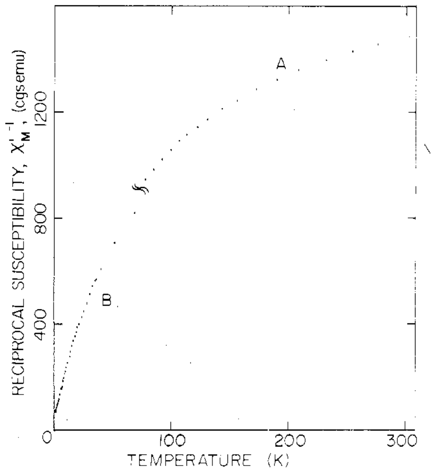

Figure 6. χ'^{-1}_M vs. T for $[(\eta^5\text{-}C_5H_5)FeS]_4PF_6$ at 5 kG. A represents data taken for $T > 50$ K with a 26.9-mg sample and B represents data taken for $T < 50$ K with a 12.0-mg sample.

metric; e.g., in the 80-kG spectrum, the outer lines are not equidistant from the center peak. This means that η is slightly less than 1, with the sense of the spectral asymmetry suggesting that the principal component of the electric field gradient is probably positive. The large asymmetry parameter results in a spectrum from which H_n can be determined quite accurately by a measurement of the separation of the outermost lines. The outer line splitting is plotted as a function of the applied field H_0 in Figure 5 for II and III. The solid lines in Figure 5 correspond to the outer line splitting obtained in computer simulations for $H_n = H_0$. In both cases the data are consistent with the effective field $H_n = H_0$ within ±3 kOe.

Magnetic Susceptibility. In Figure 6 we show the temperature dependence of the reciprocal of the molar magnetic susceptibility of the monocation (II) at 5 kG over the range 1.6 to 300 K. This plot shows that the monocation does not obey the Curie–Weiss law. It is perhaps more useful to look at the temperature dependence of the effective magnetic moment (Figure 7), as well as some sample moment data given in Table II. The moment per iron atom is observed to rise rapidly from 1.5 to 50 K and to continue increasing less rapidly with increasing T up to 300 K. Assuming spin-only behavior and $S = {}^1/_2$, i.e., one unpaired electron per monocation tetrametal cluster, the moment should be 1.73 μ_B/cluster, or 0.87 μ_B/Fe. The higher values of μ_{eff} at high T could result from the population of higher cluster spin states (e.g., $S = {}^3/_2, {}^5/_2$, etc.). Increasing moment with increasing T is also observed in III (see Table II); however, the moments at any temperature are significantly less than in II, reflecting the unpaired spin in the latter. III contains 18 metal 3d electrons and thus should be essentially diamagnetic if the energy separation of the HOMO and LUMO of this complex is large. The observed magnitude and temperature dependence of the moment suggest some population of a paramagnetic state, although a significant TIP contribution to the susceptibility cannot be ruled out and is not easily distinguished from a true population effect. The moment observed in II may be compared with some ambient-temperature effective moments per metal atom observed for the analogous paramagnetic $[(\eta^5\text{-}C_5H_5)Fe\ CO]_4{}^+$: 1.23 μ_B,[22] 1.02 μ_B,[23] and 1.10 μ_B,[24] where all of the preceding were obtained for solid samples using the Faraday method. In addition, the moment of $[(\eta^5\text{-}C_5H_5)FeCO]_4{}^+$ has also been determined for solutions using the Evans NMR method with $\mu_{eff} = 0.96\ \mu_B$.[24] Thus, while there is some variation among previously reported values of the moment for $[(\eta^5\text{-}C_5H_5)\text{-}FeCO]_4{}^+$, they are comparable with the present measurements.

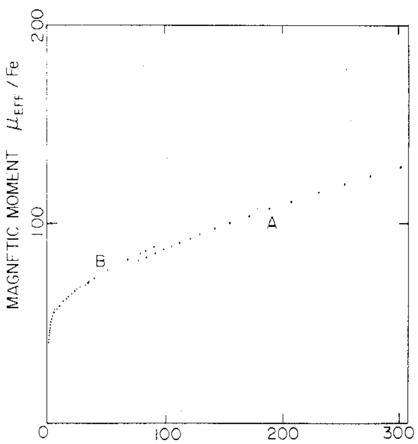

Figure 7. μ_{eff} vs. T for $[(\eta^5\text{-}C_5H_5)FeS]_4PF_6$ at 5 kG.

Table II. Sample Magnetic Moments

$[CpFeS]_4{}^+$ (II)		$[CpFeS]_4{}^{2+}$ (III)	
T, K	μ, μ_B	T, K	μ, μ_B
302.94	1.33	298.2	0.80
276.49	1.23	288.0	0.78
254.64	1.20	252.4	0.73
232.41	1.16	215.9	0.68
190.25	1.07	179.8	0.62
130.86	0.95	143.9	0.57
99.47	0.87	108.3	0.53
51.91	0.77	78.1	0.48
25.45	0.67		
11.19	0.59		
4.20	0.52		
2.14	0.45		
1.50	0.41		

The decrease in the moment of II, between 50 and 1.5 K to well below the spin-only value, may reflect intercluster exchange interactions of negative sign. Significant intercluster interactions have been observed[25] between two–four iron clusters in reduced 8-Fe ferredoxin where the clusters are 12 Å apart, although the sign of the interactions is positive. The sign and magnitude of the exchange interactions depend on the relative orientation and distance between clusters, so a negative sign in the present case is not unlikely.

Discussion

Since the Mössbauer spectra of II and III consist of single quadrupole doublets (line widths ~0.3 mm/s), we may infer that all of the iron atoms are equivalent in the oxidation level of the $[(\eta^5\text{-}C_5H_5)FeS]_4$ cluster unit within 10^{-7} s, the lifetime of the iron-57 ($I = {}^3/_2$) excited state. This most probably is also the case for the neutral species I, although the situation is obscured by the presence of what appears to be impurity in the sample. The large values of η observed in the high magnetic field spectra of II and III are consistent with the nonaxial symmetry of the iron atom sites in these structures.[20,21] Although the iron atom site parameters (e.g., Fe–S distances) change appreciably[20,21] in going from I to II to III, the electric quadrupole splittings (Table I) are virtually identical in II and III and are not significantly different from those of I. Since the quadrupole splittings reflect the distribution of charges around the iron nucleus, the combination of unchanged Fe–C (av) distances and shorter Fe–S distances,[20,21] with reduced charge in III compared to II, could fortuitously result in the same electric quadrupole splittings. In any event, Mössbauer spectroscopy apparently cannot distinguish these structures. It can, however, distinguish III from $[(CF_3)_2C_2S_2FeS]_4{}^{2-}$ (Table I), which according to ref 21 have electronically and structurally equivalent Fe_4S_4 cores. Also from Table I, we see that the values of δ and ΔE for II and III are close to those for $(Et_4N)_2[(PhCh_2S)FeS]_4$. However, reduction of the latter leads to significant changes in ΔE and δ,[15,16] whereas the change from II to III does not. Since the two systems contain different numbers of 3d electrons, the similarity of the δ and ΔE values must again be fortuitous, and the present value of δ possibly reflects a high electron density at the iron nucleus due to the bond with the electron-rich cyclopentadienyl ligand.

The invariance of the isomer shift upon oxidation from I to III suggests either that electrons are removed from ligand-based orbitals with no change of metal 3d, 4s population or that the electrons are removed from metal-based molecular orbitals in the successive oxidations of I and II and that in the resulting products, II and III, there is a redistribution of ligand electron density to the metal atoms so as to result in little overall change of metal orbital electron population. Essentially, the latter process is envisioned in a recent molecular orbital study[26] of a number of ligand-bridged $[Fe_2(CO)_6X_2]$ dimers exhibiting metal–metal interactions. These systems exist in 0, –1, and –2 oxidation levels, and upon reduction through this sequence there is little change in the isomer shift.

In zero field, in the limit of slow relaxation, magnetic hyperfine splitting, or at least broadening, is expected for spin density localized on the iron sites. The fact that neither splitting nor broadening is observed at 4.2 K therefore suggests either rapid paramagnetic relaxation or little spin density at the iron sites. In the former case, we would expect to observe a magnetic hyperfine interaction in addition to the direct effect of the applied field on the nucleus because at low temperatures the applied field will polarize the unpaired spin, giving rise to a magnetic hyperfine field, H_{hf}. The observed field at the nucleus is $\mathbf{H}_n = \mathbf{H}_{hf} + \mathbf{H}_o$, where H_o is the applied field. According to Freeman and Watson,[27] one unpaired d electron produces a contact hyperfine field of $\sim$–120 kOe at the iron nucleus. Since the unpaired electron is localized on one individual iron site for a short time compared to the Larmor precession time, we expect to observe at least $\mathbf{H}_{hf} \approx -30$ kG at each of the four sites, an easily measured effect. The fact that $H_n = H_o$ (i.e., $H_{hf} = 0 \pm 3$ kOe) for II and III (Figure 4) strongly suggests that the unpaired spin in II does not interact with the iron sites and presumably occupies a predominantly ligand-based molecular orbital.

Dahl and co-workers have proposed qualitative and quantitative MO bonding schemes [21,24,26,28] which seek to rationalize the properties of the various clusters. The qualitative scheme assumes that the metal–bridge and metal–ligand interactions can be separated from metal–metal interactions. In the case of the innocent terminal ligands such as mercaptides, the tetrametal orbitals generated from the metal–metal interaction lie highest in energy and factor into bonding, nonbonding, and antibonding orbitals. For species such as $[Fe_4S_4(SR)_4]^{2-}$, the electron added upon reduction goes into a nonbonding tetrametal orbital producing a "high-spin" cluster system. In the case of noninnocent terminal ligands such as cyclopentadienyl, the metal–ligand interaction mixes the tetrametal and ligand orbitals. The redox electrons fill metal ligand orbitals which are of predominantly ligand nature, and odd electron configurations are "low spin". The results of this work suggest that the sulfur compounds I, II, and III are very similar to the previously studied carbonyl analogues in this respect. The unexpected intercluster magnetic interactions of the monocation cluster (II) are presently under further investigation.

Acknowledgment. We are grateful to L. Dahl, K. Johnson, M. Hall, and B. K. Teo for useful discussions of the theoretical aspects of these systems. T.J.M. acknowledges the support of the National Science Foundation, Grant No. GP-17083. W.M.R. acknowledges the support of the National Science Foundation, Division of Materials Research, Solid State Chemistry Program, Grant No. DMR 75-13592A01. He also acknowledges the partial support of the Research Corporation and H.E.W. Grant No. RR07143. The Francis Bitter National Magnet Laboratory is supported by the National Science Foundation.

Registry No. I, 64314-90-5; II·PF_6, 64653-28-7; III·$(PF_6)_2$, 64653-27-6.

References and Notes

(1) C. W. Carter, Jr., J. Kraut, S. T. Freer, R. A. Alden, L. C. Sieker, E. Adman, and L. H. Jensen, *Proc. Natl. Acad. Sci. U.S.A.*, **69**, 3526 (1972).
(2) E. T. Adman, L. C. Sieker, and L. H. Jensen, *J. Biol. Chem.*, **248**, 3987 (1973).
(3) K. Gersonde, H. E. Schlaak, M. Breitenbach, F. Parak, H. Eicher, W. Zgorzalla, M. G. Kalvius, and A. Mayer, *Eur. J. Biochem.*, **43**, 307 (1974).
(4) C. L. Thompson, C. E. Johnson, D. P. E. Dickson, R. Cammack, D. O. Hall, U. Weser, and K. K. Rao, *Biochem. J.*, **139**, 97 (1974).
(5) D. P. E. Dickson, C. E. Johnson, R. Cammack, M. C. W. Evans, D. O. Hall, and K. K. Rao, *Biochem. J.*, **139**, 105 (1974).
(6) J. C. M. Tsibris and R. W. Woody, *Coord. Chem. Rev.*, **5**, 417 (1970).
(7) C. H. Wei,, G. R. Wilkes, P. M. Treichel, and L. F. Dahl, *Inorg. Chem.*, **5**, 900 (1966).
(8) M. A. Neumann, Trinh-Toan, and L. F. Dahl, *J. Am. Chem. Soc.*, **94**, 3383 (1972).
(9) A. L. Balch, *J. Am. Chem. Soc.*, **91**, 6962 (1969).
(10) I. Bernal, B. R. Davis, M. L. Good, and S. Chandra, *J. Coord. Chem.*, **2**, 61 (1972).
(11) T. Herskovitz, B. A. Averill, R. H. Holm, J. A. Ibers, W. D. Phillips, and J. F. Weiher, *Proc. Natl. Acad. Sci. U.S.A.*, **69**, 2437 (1972).
(12) B. A. Averill, T. Herskovitz, R. H. Holm, and J. A. Ibers, *J. Am. Chem. Soc.*, **95**, 3523 (1973).
(13) R. H. Holm, W. D. Phillip, B. A. Averill, J. J. Mayerle, and T. Herskovitz, *J. Am. Chem. Soc.*, **96**, 2109 (1974).
(14) B. V. DePamphilis, B. A. Averill, T. Herskovitz, L. Que, Jr., and R. H. Holm, *J. Am. Chem. Soc.*, **96**, 4159 (1974).
(15) R. B. Frankel, T. Herskovitz, B. A. Averill, R. H. Holm, P. J. Krusic, and W. D. Phillips, *Biochem. Biophys. Res. Commun.*, **58**, 974 (1974).
(16) R. B. Frankel, B. A. Averill, and R. H. Holm, *J. Phys. (Paris), Colloq.*, **35**, 6–75 (1974).
(17) R. B. Frankel, W. M. Reiff, I. Bernal, and M. L. Good, *Inorg. Chem.*, **13**, 493 (1974).
(18) P. Greatrex and N. N. Greenwood, *Discuss. Faraday Soc.*, **47**, 126 (1969).
(19) R. B. Frankel, W. M. Reiff, T. J. Meyer, and J. L. Cramer, *Inorg. Chem.*, **13**, 2515 (1974).
(20) Trinh-Toan, W. P. Fehlhammer, and L. F. Dahl, *J. Am. Chem. Soc.*, **99**, 402 (1977).
(21) Trinh-Toan, B. K. Teo, J. A. Ferguson, T. J. Meyer, and L. F. Dahl, *J. Am. Chem. Soc.*, **99**, 408 (1977).
(22) J. A. Ferguson and T. J. Meyer, *J. Am. Chem. Soc.*, **94**, 3409 (1972).
(23) R. B. King, *Inorg. Chem.*, **5**, 2227 (1966).
(24) Trinh-Toan, W. P. Fehlhammer, and L. F. Dahl, *J. Am. Chem. Soc.*, **94**, 3389 (1972).
(25) R. Matthews, S. Charltan, R. H. Sands, and G. Palmer, *J. Biol. Chem.*, **249**, 4326 (1974).
(26) B. K. Teo, M. B. Hall, R. F. Fenske, and L. F. Dahl, *Inorg. Chem.*, **14**, 3103 (1975).
(27) A. J. Freeman and R. E. Watson in "Magnetism", Vol. IIA, G. T. Rado and H. Suhl, Ed., Academic Press, New York, N.Y., 1965, Chapter 2.
(28) R. S. Gall, C. T. W. Chu, and L. F. Dahl, *J. Am. Chem. Soc.*, **96**, 4019 (1974).